TRENDS IN SCIENCES 2025; 22(12): 10852
https://doi.org/10.48048/tis.2025.10852 RESEARCH ARTICLE

Comparative Analysis of Mitragynine and Alkaloid Content in Cultivated *M. speciosa* Leaves and Their α-Glucosidase Inhibitory Activity

Netnapa Chana[1,2], Jamjan Pechsiri[3], Parichat Thepthong[2,4], Ratanaporn Pakee[4], Witsuta Decha[4] and Panita Kongsune[2,4,*]

[1]*Department of Biological Science, Faculty of Science and Digital Innovation, Thaksin University, Phattalung 93210, Thailand*
[2]*Innovative Material Chemistry for Environment Center, Department of Chemistry, Faculty of Science, Thaksin University, Phattalung 93210, Thailand*
[3]*Modern of Agricultural Science, Faculty of Technology and Community Development, Thaksin University, Phattalung 93210, Thailand*
[4]*Department of Physical Science, Faculty of Science and Digital Innovation, Thaksin University, Phattalung 93210, Thailand*

([*]Corresponding author's e-mail: dpanita@tsu.ac.th)

Received: 5 June 2025, Revised: 19 July 2025, Accepted: 26 July 2025, Published: 10 September 2025

Abstract

Mitragyna speciosa (kratom) is a Southeast Asian medicinal plant rich in indole and oxindole alkaloids, with mitragynine as its major bioactive component. However, the influence of propagation method, variety, and leaf maturity on alkaloid biosynthesis remains underexplored. This study conducted a comparative analysis of total alkaloid and mitragynine content in kratom leaves from 3 varieties - green vein, red vein, and "Hang Kang" - propagated by seed or stem cutting and harvested at 2 maturity stages (4^{th} and 6^{th} leaf pairs). Methanolic extracts yielded the highest alkaloid levels, and mitragynine was isolated and structurally confirmed by HPLC, ^{1}H NMR, and ^{13}C NMR spectroscopy. Quantitative results showed that seed-propagated semi-mature leaves of the Hang Kang variety (HK-S-seed) contained the highest total alkaloids (1.59 %w/w) and mitragynine (10.37%, or 103.70 mg/g alkaloid extract). Additionally, α-glucosidase inhibitory assays revealed strong activity of mitragynine (IC_{50} = 48.09 µg/mL), exceeding that of acarbose on a µg/mL basis. Molecular docking further supported these findings, showing high binding affinities of mitragynine and related alkaloids (−9.84 to −11.87 kcal/mol). Collectively, the results highlight the impact of cultivation variables on bioactive compound accumulation and suggest the potential of mitragynine as a natural scaffold for α-glucosidase inhibition.

Keywords: Kratom, Mitragynine, Alkaloid content, Propagation method, α-glucosidase inhibition, Molecular docking

Introduction

Mitragyna speciosa Korth. (Rubiaceae), or *M. speciosa* commonly known as kratom, is a medicinal plant indigenous to Southeast Asia, particularly Thailand, Malaysia, and Indonesia. Traditionally, kratom leaves have been used as stimulants in low doses and sedatives in high doses, with additional applications in pain relief, diarrhea treatment, and management of opioid withdrawal symptoms [1-3]. In recent years, increasing scientific attention has been directed toward the plant's chemical constituents, especially its rich profile of indole, oxindole alkaloids, and mitragynine which underlie many of its bioactive compound profiles [4-7]. While kratom is taxonomically classified as a single species (*Mitragyna speciosa*), traditional cultivators often distinguish different strains based on morphological features such as leaf shape, vein color,

and growth pattern, which may be linked to differences in alkaloid content [8]. The most commonly recognized vein types - green and red - are typically associated with differing bioactivities. Green vein kratom is often described as moderately stimulating and analgesic, whereas red vein kratom is associated with sedative and pain-relieving effects. In southern Thailand, several indigenous landraces have been identified based on local cultivation practices and traditional knowledge. Among them, the "Hang Kang" cultivar - named after the mantis shrimp's tail due to its distinct morphology - is widely grown in provinces such as Nakhon Si Thammarat and Phatthalung. This landrace is reputed for its vigorous growth and high, consistent mitragynine yield [9].

Mitragynine accounts for approximately 60% of the total alkaloid content in kratom leaves and has demonstrated diverse bioactivities including analgesic, anti-inflammatory, antioxidant, and antidiabetic effects [7,10,11]. Type 2 diabetes mellitus (T2DM) is a chronic metabolic disorder characterized by postprandial hyperglycemia resulting from impaired glucose metabolism. Inhibitors of α-glucosidase, an enzyme that catalyzes the hydrolysis of carbohydrates into glucose, are effective in delaying glucose absorption and reducing blood sugar spikes. Current synthetic drugs such as acarbose are clinically used but often associated with gastrointestinal side effects, prompting the search for safer alternatives from natural sources [12]. Notably, mitragynine has been identified as a natural inhibitor of α-glucosidase - an enzyme involved in carbohydrate digestion - suggesting its potential in managing postprandial hyperglycemia in type 2 diabetes [13-15]. The α-glucosidase inhibitory activity of mitragynine and related extracts has been demonstrated *in vitro* with moderate potency compared to standard drugs such as acarbose [14,15]. In support of these findings, *in silico* molecular docking studies have revealed strong binding affinities between mitragynine and α-glucosidase active sites, primarily involving hydrogen bonding with key catalytic residues such as Asp327, Arg526, Asp542, and His600 [13,16]. These results provide mechanistic insights into the enzyme-inhibitory potential of mitragynine and support its development as a functional nutraceutical.

While previous studies have focused on the pharmacological activities of mitragynine and its analogs, less attention has been given to the variability of its content within the plant under different cultivation conditions. Factors such as kratom variety, propagation method, and leaf maturity may influence alkaloid biosynthesis and accumulation, thereby affecting the quality and consistency of kratom-derived products. Understanding these variations is critical for optimizing cultivation practices and ensuring reliable phytochemical yields for medicinal and industrial applications. Emerging evidence suggests that secondary metabolite biosynthesis in kratom is affected by multiple variables [17]. Recent studies suggest that multiple factors - including genetic variation among cultivars, propagation methods (e.g., seed versus cutting), leaf developmental stage, and environmental conditions such as light intensity, soil moisture, pH, and calcium levels - may influence mitragynine biosynthesis [9,18-20]. For instance, Leksungnoen *et al*. [18] found that moderate water stress combined with low light intensity enhanced mitragynine accumulation in kratom leaves. Additionally, Laforest *et al*. [9] reported that mitragynine content varies among different cultivars and developmental stages, with mature leaves exhibiting higher concentrations. Chongdi *et al*. [19] further highlighted those regional environmental factors, such as soil nutrients and light availability, significantly affect kratom growth and alkaloid profiles. Moreover, the alkaloid content in kratom diverges based on seasonal and geographical origin Sengnon *et al*. 2023. Despite increasing interest in the pharmacological properties of kratom, little is known about how cultivation parameters such as variety, propagation method, and leaf maturity influence mitragynine content and bioactivity. This lack of comparative data hinders the development of standardized kratom-based products.

Therefore, this study aims to (1) compare total alkaloid and mitragynine content in 3 kratom varieties - green vein, red vein, and the indigenous "Hang Kang" cultivar - propagated by seed and stem cutting, and harvested at 2 leaf maturity stages (semi-mature and mature), and (2) evaluate the α-glucosidase inhibitory activity of mitragynine and other alkaloids through *in vitro* assays and molecular docking. Extraction, purification, and HPLC quantification of mitragynine were performed alongside *in vitro* enzyme inhibition assays and docking simulations to assess binding

affinity and interaction mechanisms. The novelty of this work lies in integrating alkaloid quantification with *in vitro* and *in silico* enzyme inhibition studies to identify optimal cultivation strategies for future pharmacological applications.

Materials and methods

Materials and *M. speciosa* leaves extraction

All analytical grade chemicals were purchased from Sigma-Aldrich (Burlington, MA, USA) and reagents were obtained from Merck. Fresh leaves of *Mitragyna speciosa* leaves (green-veined, red-veined, and Hang Kang varieties) were collected from authenticated sources in a local community enterprise in Nakorn Si Thammarat Province, Thailand. The leaves were cleaned, dried at 60 °C for 2 days, and ground into a fine powder. The extraction was performed using maceration with dichloromethane, ethyl acetate, and methanol at room temperature for 3 - 5 days. The solvent was evaporated under reduced pressure to obtain the crude extracts. After filtration, the solvents were evaporated under reduced pressure.

Isolation of alkaloids and purification of mitragynine

To isolate the alkaloids, the methanol crude extract underwent silica gel column chromatography using 2% methanol in dichloromethane as the eluent to obtain the alkaloid fraction, which was monitored by TLC under UV light and Dragendorff's reagent. The fraction was then dissolved in 10% acetic acid, thoroughly shaken, and left overnight. The acidic solution was washed with petroleum ether, adjusted to pH 9 with 25% ammonia, and extracted with chloroform. The chloroform phase was partitioned with distilled water, dried over anhydrous sodium sulfate, and evaporated to yield the crude alkaloid extract (AE) [6].

The AE extract was further purified using silica gel column chromatography with 5% methanol in dichloromethane as the eluent, yielding mitragynine as an amorphous powder. The structure of mitragynine was elucidated using 1-dimensional (1D) and 2-dimensional (2D) Nuclear Magnetic Resonance (NMR) spectroscopy and further validated by High-Performance Liquid Chromatography (HPLC) analysis. The purified mitragynine was subsequently used as a standard for the quantitative analysis of mitragynine.

Quantitative analysis of Mitragynine by HPLC

A mitragynine standard was prepared in HPLC-grade methanol at various concentrations for calibration curve construction. The AE fraction (1 mg/mL) of each sample was analyzed using an Agilent 1260 HPLC system [21]. Details of the 3 kratom varieties - green vein, red vein, and the local "Hang Kang" cultivar - grown via seed propagation and stem cutting at 2 maturity stages (semi-mature and mature). Methanol (100%) was used as both the sample diluent and the solvent for the reference standard. The mobile phase consisted of 2 solvents: Mobile Phase A was 5.0 mM ammonium bicarbonate buffer adjusted to pH 9.50, and Mobile Phase B was acetonitrile. Chromatographic separation was carried out using a C18 reversed-phase column (250×4.6 mm^2, 5 µm particle size) at a flow rate of 1.0 mL/min. Detection was performed at 254 nm, with an injection volume of 10 µL. The column temperature was maintained at 25 °C throughout the analysis [21].

α-Glucosidase inhibitory assay

The inhibitory activity of the crude extracts against α-glucosidase was determined using a spectrophotometric assay. The enzyme catalyzes the hydrolysis of p-nitrophenyl-α-D-glucopyranoside (PNP-G) into p-nitrophenol and glucose (Scheme S1), producing a yellow color detectable at 405 nm. A reduction in absorbance indicates enzyme inhibition by the extract. The reaction mixture in a 96-well microplate contained 8 U/mL α-glucosidase, 5.0 mM PNP-G, phosphate buffer (pH 6.8), and varying concentrations of crude extracts (10 - 150 µg/mL) [22]. Acarbose was used as a positive control. The percentage inhibition was calculated, and IC_{50} values were determined via linear regression analysis.

Molecular docking

The crystal structures of α-glucosidase complexed with miglitol (PDB ID: 3L4W; resolution: 2.00 Å, R-free: 0.232, R-work: 0.198 [23]) and acarbose (PDB ID: 7DCH; resolution: 1.69 Å, R-free: 0.203, R-work: 0.177 [24]) were obtained from the Protein Data Bank (PDB) [25]. Protein preparation involved the removal of water molecules and addition of hydrogen atoms to stabilize the structure for docking analysis. The compounds of *M. speciosa*, were drawn in GaussView [26] and geometry-

optimized using Hartree-Fock/6-31G** level theory via Gaussian 03 [27]. Optimized structures were exported in .pdb format for subsequent docking analysis. Docking simulations were carried out using AutoDock 4.2 [28]. Ligands were treated as flexible (torsion enabled), while protein structures were kept rigid. Gasteiger–Marsili charges [29] were assigned to all atoms using AutoDock Tools [30], and all files were converted to .pdbqt format. The free binding energy (ΔG) was computed using an empirical scoring function incorporating various interaction terms, expressed as $\Delta G = \Delta G_{vdw} + \Delta Gh_{bond} + \Delta G_{elec} + \Delta G_{tor} + \Delta G_{sol}$, where ΔG_{vdw}, where ΔGvdw accounts for van der Waals forces, ΔGhbond for hydrogen bonding, ΔGelec for electrostatic interactions, ΔGtor for the entropic penalty due to torsional restriction, and ΔGsol for solvation and hydrophobic effects [31]. To validate the docking procedure, known inhibitors miglitol and acarbose were re-docked into the α-glucosidase active site to benchmark the docking accuracy. The binding energy values obtained for miglitol and acarbose served as reference points for subsequent screening and evaluation of alkaloid and flavonoid compounds derived from *M. speciosa* extracts.

Statistical analysis

All experiments were performed in triplicate. Data analysis used one-way ANOVA with Duncan's test ($p < 0.05$). Results are presented as mean ± SD. Statistical analysis was performed using SPSS software.

Results and discussion

Mitragynine isolation and characterization

Extraction of *M. speciosa* leaves yielded different percentages depending on the solvent used. The crude methanolic extract showed the highest yield (8.18 %w/w), followed by the dichloromethane (2.37 %w/w) and ethyl acetate extracts (0.95 %w/w). These findings are in agreement with previous studies that reported methanol as the most effective solvent for extracting alkaloids from kratom leaves, producing mitragynine yields of approximately 1.6 %w/w from dry leaves [4]. These results highlight the polarity-dependent extraction efficiency, with methanol effectively extracting polar constituents and dichloromethane and ethyl acetate targeting less polar compounds. Therefore, in this study, the crude methanolic extract was subjected to alkaloid extraction. The presence of alkaloids was confirmed using Dragendorff's reagent. The alkaloid yield was 0.16% based on the original plant material. When calculated relative to the crude methanolic extract, the alkaloid content increased to 2.02% of the crude extract. Therefore, methanol was selected as the solvent for extracting mitragynine to be used as a reference standard and for further extraction in studying the effects of variety and leaf pair type on the alkaloid and mitragynine contents.

The alkaloid extract was subjected to the isolation of mitragynine. The structure of mitragynine was confirmed using ^{1}H NMR (400 MH_z, $CDCl_3$) and ^{13}C NMR (100 MH_z, $CDCl_3$) [32] spectroscopy as shown in **Table 1**. The ^{1}H NMR spectrum displayed characteristic chemical shifts corresponding to the functional groups present in the alkaloid structure. A broad singlet at δH 7.82 was assigned to the NH proton, confirming the presence of the indole moiety. The presence of aromatic protons was identified at δH 6.45 (d), 6.98 (t), and 6.90 (d), which aligned with the expected resonances for the methoxy-substituted indole ring system. Signals at δH 3.04 (m), 3.14 (m), and 2.95 (m) were assigned to aliphatic methylene groups, while δH 1.62 (d) and 1.21 (m) corresponded to methyl-bearing carbons. The presence of methoxy groups was confirmed by singlets at δH 3.87 and 3.75, consistent with OCH_3 functional groups.

The ^{13}C NMR spectrum provided further structural validation. The signal at δC 160.67 confirmed the presence of the aromatic carbon bonded to a nitrogen group, characteristic of the indole framework. The aliphatic carbons were observed at δC 40.62, 39.62, and 29.93, while the methyl groups appeared at δC 12.88 and 19.04. The methoxy carbon signals were detected at δC 61.66 and 55.42, aligning well with expected chemical shifts.

Table 1 The ^{1}H NMR and ^{13}C NMR chemical shifts of mitragynine isolated from *M. speciosa* leaves ($CDCl_3$, 400 MHz for ^{1}H NMR and 100 MHz for ^{13}C NMR) compared with reference values [32] (parentheses).

Position	Chemical shift signals δ (ppm)		Type	Position	Chemical shift signals δ (ppm)		Type
	^{13}C NMR	^{1}H NMR			^{13}C NMR	^{1}H NMR	
		7.82 (7.74), *bs*	NH	20	40.62, (40.7)	1.62, (1.64), *dt*	CH
3	61.41, (61.3)	3.04, (3.20), *m*	CH	21	53.63, (57.7)	3.12, (3.00), *m*	CH_2
5	57.97, (53.8)	3.14, (2.97), *m*	CH_2	9-OCH_3	55.42, (55.5)	3.75, (3.87), *s*	OCH_3
6	23.94, (23.9)	2.95, (3.11), *m*	CH_2	17-OCH_3	61.66, (61.7)	3.87, (3.73), *s*	OCH_3
10	99.74, (99.9)	6.45, (6.45), *d*	CH	22-OCH_3	51.37 (51.5)	3.71 (3.71), s	OCH_3
11	111.40, (122)	6.98, (7.0), *t*	CH				
12	104.25, (104.3)	6.90, (6.90), *d*	CH				
14	29.93, (30.0)	1.78, (2.55), *s*	CH_2				
15	39.62, (39.9)	2.50, (3.06), *s*	CH				
17	160.67, (169.4)	7.42, (7.43), *s*	CH				
18	12.88 (13.0)	0.84 (0.87), *t*	CH_3				
19	19.04, (19.3)	1.21, (1.19), *m*	CH_2				

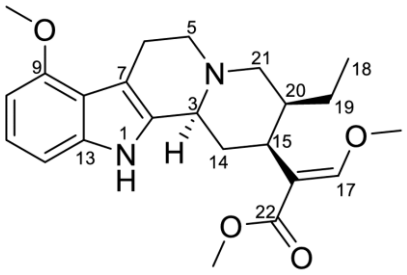

Mitragynine structure

High-Performance Liquid Chromatography **(**HPLC**)** was used to further confirm the presence of mitragynine. The chromatogram displayed a prominent peak at retention time 9.716 min (MG), which corresponds to the reference standard of mitragynine. An internal standard (IS) appeared at 4.580 min, ensuring the reliability of the retention time measurement. The separation was carried out under optimized chromatographic conditions, confirming the identity and purity of the mitragynine peak. The HPLC analysis demonstrated a well-resolved peak for mitragynine without significant interference from other compounds, suggesting the method's high specificity. The peak's retention time and area were consistent with reported values, reinforcing the structural assignment of mitragynine.

Comparative alkaloid and mitragynine profiles

Quantitative analysis of mitragynine content was conducted on 3 kratom leaf types: red vein, green vein, and "Hang Kang" variety. Each type was cultivated using 2 propagation methods - seed propagation and stem cutting. Leaf samples were collected from the 4th and 6th leaf pairs at the Ban Nua Nam community enterprise farm in Cha-uat District, Nakhon Si Thammarat Province. Sample details are summarized in **Table 2**. The analysis was performed in triplicate using HPLC [21]. Standard curves were prepared from mitragynine solutions at concentrations of 2.00, 4.00, 8.00, 20.00, 50.00 and 100.00 ppm. The resulting chromatograms (**Figure 1**) confirmed sharp and well-resolved mitragynine peaks without interference, indicating high selectivity of the analytical method. Method validation demonstrated excellent linearity (R^2 > 0.999958), precision (RSD < 2%), and accuracy (recovery between 98% - 102%). This study focused on comparing the methanolic extract yield, total alkaloid content, and mitragynine levels across the 3 kratom varieties under different propagation methods and leaf ages.

Table 2 Presents the (A) details of kratom leaf samples, including the type of leaf/planting method, leaf characteristics/node pair, and sample codes for each type and B) nomenclature used in the study.

(A) Kratom leaf sample codes and descriptions			**(B) Nomenclature and abbreviations**	
Leaf type / planting method	**Leaf pair (Maturity)**	**Sample code**	**Abbreviation**	**Definition**
Green vein from stem cutting	4th (Semi-mature)	G-S-stem	AE	Alkaloid extract
	6th (Mature)	G-M-stem	BE	Binding energy (kcal/mol)
Green vein from seed propagation	4th (Semi-mature)	G-S-seed	%DS	Percentage of Docking Score
	6th (Mature)	G-M-seed	IC_{50}	50% Inhibitory Concentration
Red vein from stem cutting	4th (Semi-mature)	R-S-stem	IS	Internal Standard
	6th (Mature)	R-M-stem	MG	Mitragynine
Red vein from seed propagation	4th (Semi-mature)	R-S-seed	NMR	Nuclear Magnetic Resonance
	6th (Mature)	R-M-seed	PNP-G	Nitrophenyl-α-D-
Hang Kang from stem cutting	4th (Semi-mature)	HK-S-stem		p- glucopyranoside
	6th (Mature)	HK-M-stem	RMSD	Root-Mean-Square Deviation
Hang Kang from seed propagation	4th (Semi-mature)	HK-S-seed	RT	Retention Time (min)
	6th (Mature)	HK-M-seed	PDB	Protein Data Bank

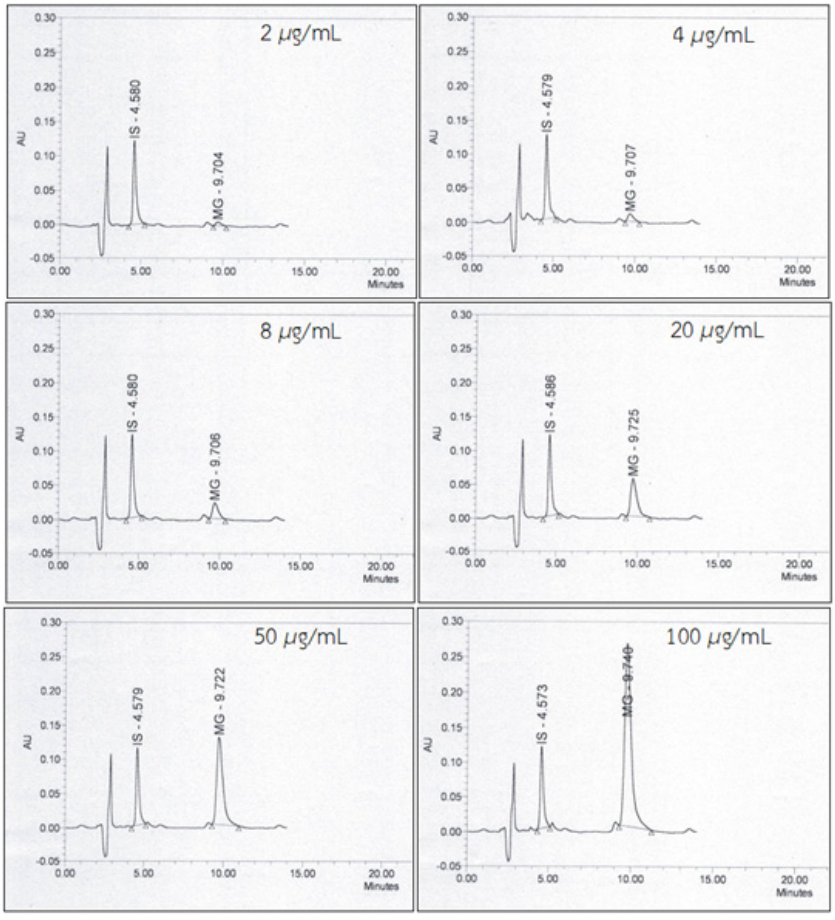

Figure 1 HPLC chromatograms of mitragynine at concentrations ranging from 2 to 100 µg/mL.

The analytical results presented in **Figure 2** reveal distinct variations in methanol extract yield, total alkaloid content, and mitragynine concentration among different kratom varieties, propagation methods, and leaf maturities. The extraction yields of ethanol and alkaloid extracts from various kratom leaf samples (**Table 2**) are presented in **Figure 2**. Among all samples, the Hang Kang variety demonstrated the highest ethanol extract yields, particularly in the HK-M-seed (11.28%), HK-M-stem (10.95%), and HK-S-stem (10.25%) samples (**Figure 2(a)**). In contrast, the green vein and red vein samples showed lower ethanol yields, ranging from approximately 3.94% to 9.19%. The increased ethanol extract yield observed in the Hang Kang variety suggests a greater abundance of ethanol-soluble phytochemicals, potentially influenced by genetic background and seed propagation method. Similarly, alkaloid extraction yields (**Figure 2(b)**) exhibited a comparable pattern. The green vein samples, particularly G-S-stem (1.93%) and G-S-seed (1.64%), displayed relatively high alkaloid yields compared to the red vein samples, such as R-S-seed (0.21%) and R-M-seed (0.58%). The Hang Kang samples maintained moderate alkaloid yields, with HK-S-seed achieving 1.59%. These differences indicate that both the type of vein and the propagation method significantly impact alkaloid accumulation in kratom leaves.

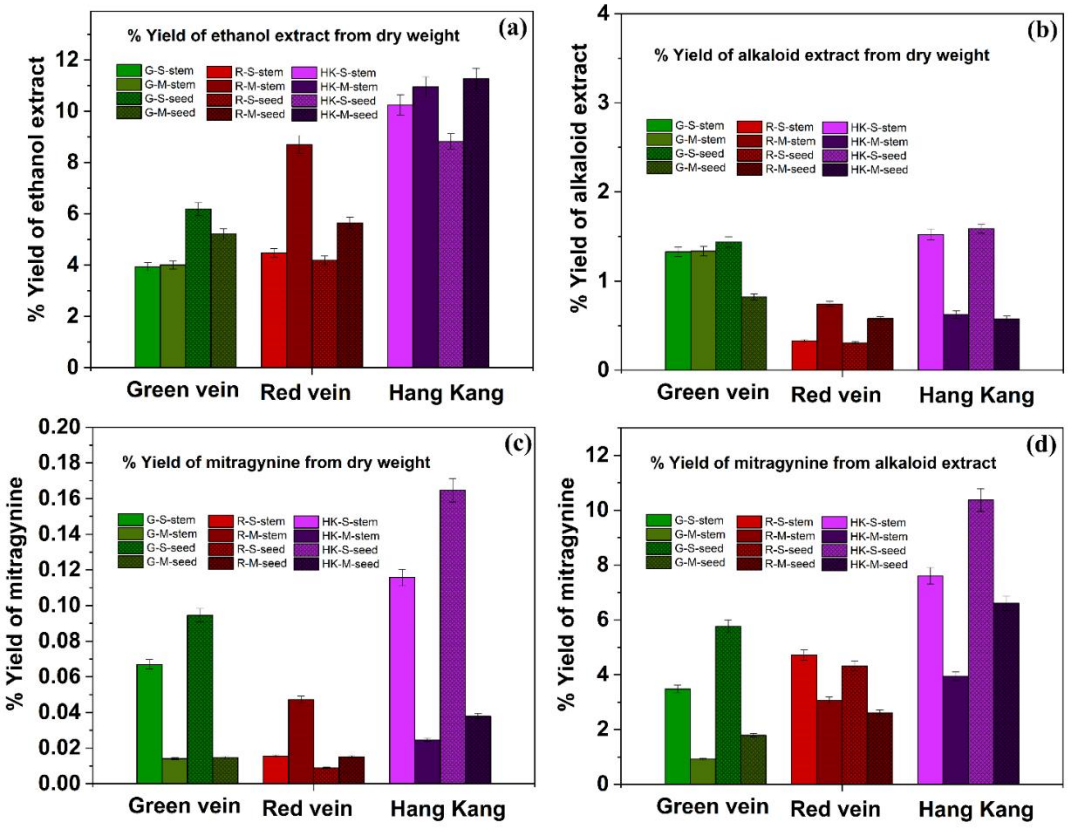

Figure 2 Comparison of % yield of (a) ethanol extract, (b) alkaloid extract, (c) mitragynine from dry weight and (d) % yield of mitragynine from alkaloid extract.

The yield of mitragynine from the alkaloid extracts varied notably among the samples (**Figure 2(c)**). The highest mitragynine yield was observed in HK-S-seed (10.37%), followed by HK-S-stem (7.61%) and G-S-seed (5.76%). In contrast, the lowest yields were found in G-M-stem (0.92%) and R-M-seed (2.61%). When the mitragynine content was normalized per gram of alkaloid extract (**Figure 2(d)**), HK-S-seed exhibited the highest concentration (103.70 mg/g alkaloid), followed by HK-S-stem (76.05 mg/g) and G-S-seed (57.64 mg/g). Red vein samples showed generally lower mitragynine contents, suggesting a vein-dependent variation in alkaloid profiles.

The Hang Kang variety consistently exhibited higher alkaloid and mitragynine levels than green or red vein types, regardless of propagation method. For example, HK-S-seed showed the highest mitragynine content (10.37% of alkaloid extract), while R-M-seed had the lowest (2.61%). These results support the use of phytochemical profiles for varietal differentiation and suggest genetic influences on biosynthesis. Moreover, seed-propagated plants generally showed higher alkaloid accumulation than those from stem cuttings. Additionally, semi-mature leaves tended to contain more mitragynine than mature ones, indicating developmental stage-dependent biosynthesis. These findings align with previous reports that stress, age, and light exposure influence alkaloid production in kratom [18-20]. The genotypic factors and propagation techniques influence the expression of enzymes involved in indole alkaloid biosynthesis [9]. In particular, seed-propagated kratom plants have been reported to exhibit higher alkaloid yields due to enhanced secondary metabolic pathways compared to those propagated via stem cuttings [17]. Moreover, cultivar-dependent traits such as leaf structure, metabolic rate, and responsiveness to environmental cues may also explain the observed variations among kratom types [18].

The reliability of the findings is strengthened by the linearity of the HPLC calibration curve and the clarity of mitragynine peaks in the chromatograms. Consistent sample collection from a single cultivation site also minimized variability. These findings provide meaningful insights into the effects of variety, propagation method, and leaf maturity on bioactive compound production in *Mitragyna speciosa*, supporting the optimization of cultivation strategies for industrial and pharmacological applications.

α-Glucosidase inhibitory activity

Mitragyna speciosa has attracted increasing attention due to its diverse pharmacological properties, particularly its potential antidiabetic effects. In this study, the α-glucosidase inhibitory activities of mitragynine, alkaloid extract, crude methanol extract, ethyl acetate extract, dichloromethane extract, and the standard drug acarbose were evaluated through dose-response assays (**Figure 3**), and their IC_{50} values were calculated and summarized in **Table 3**.

Among the tested samples, mitragynine exhibited the highest inhibitory activity with an IC_{50} of 48.09 μg/mL (120.70 μM), followed by the alkaloid extract (IC_{50} = 52.91 μg/mL), which consists of mitragynine and other structurally related indole alkaloids. The relatively strong inhibition observed in the alkaloid extract suggests potential synergistic interactions among these compounds. The crude methanol extract, which includes a broader range of polar and semi-polar phytochemicals, also demonstrated significant inhibition (IC_{50} = 66.72 μg/mL), implying that other non-alkaloid constituents may contribute to the overall activity. In contrast, the ethyl acetate and dichloromethane extracts showed comparatively lower inhibitory effects, with IC_{50} values of 78.33 and 103.71 μg/mL, respectively, indicating a reduced presence of active compounds in these less polar fractions.

When compared to acarbose (IC_{50} = 61.62 μg/mL or 95.45 μM), mitragynine was slightly less potent on a molar basis (120.70 μM), although it remains noteworthy due to its natural origin and potential for structural optimization. All dose-response curves demonstrated strong linear correlations (R^2 values ranging from 0.9131 to 0.9777), validating the reliability of the observed inhibitory trends.

The mitragynine content in the seed-propagated Hang Kang cultivar (103.70 mg/g extract) is notably higher than that reported by Laforest *et al.* [9], who observed values ranging from 55 to 87 mg/g across various landraces. This difference may be attributed to differences in propagation methods and leaf developmental stages. Similarly, the observed IC_{50} value for mitragynine (48.09 μg/mL) against α-glucosidase is more potent than the 65.3 μg/mL reported by Chongdi *et al.* [19], possibly due to higher compound purity and extraction optimization in this study. Overall, these findings underscore the potential of *Mitragyna speciosa*, particularly its alkaloid constituents such as mitragynine, as promising candidates for the development of bio-based functional compounds aimed at managing postprandial hyperglycemia in type 2 diabetes.

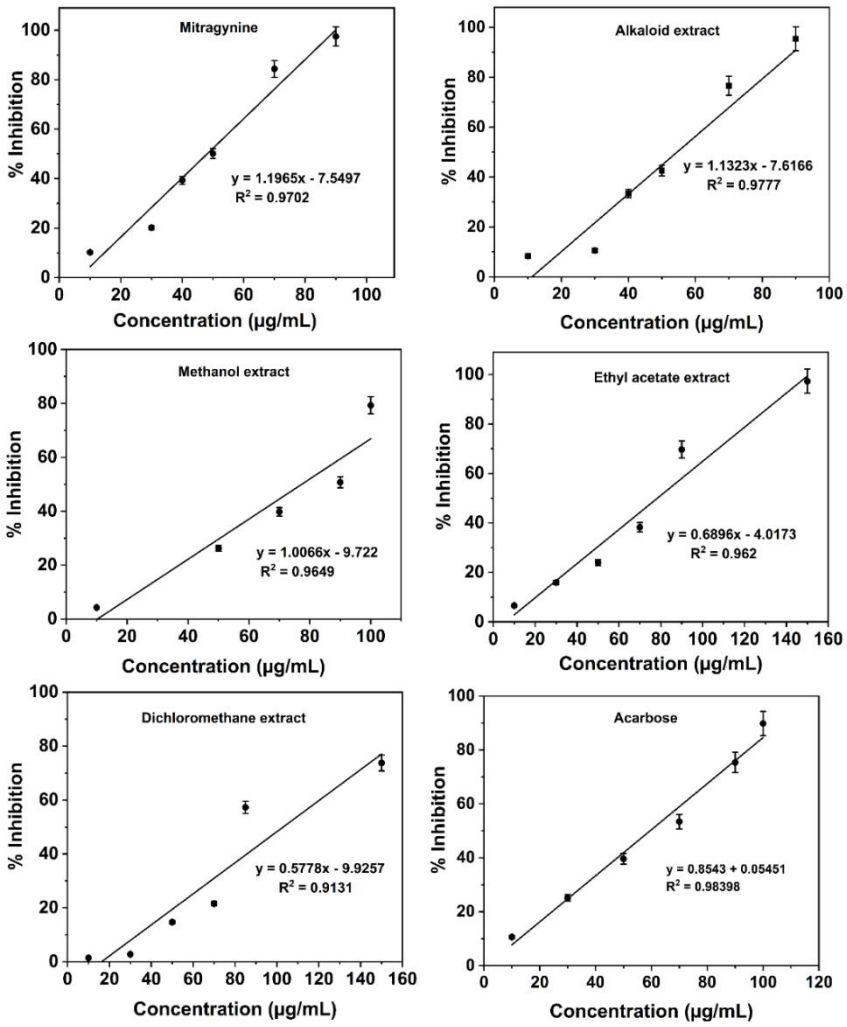

Figure 3 α-Glucosidase inhibitory activity of mitragynine, alkaloid extract, methanol extract, ethyl acetate extract, dichloromethane extract, and acarbose (standard).

Table 3 presents the IC_{50} values for α-glucosidase inhibition of mitragynine, alkaloid extract, crude methanol extract, dichloromethane extract, ethyl acetate extract, and the standard drug acarbose.

Samples	IC_{50}	
	µg/mL:8U/mL	**(µM)**
Mitragynine	48.09 ± 0.22	120.70 ± 0.22
Alkaloid extract	52.91 ± 0.33	-
Methanol extract	66.72 ± 0.23	-
Ethyl acetate extract	78.33 ± 0.26	-
Dichloromethane extract	103.71 ± 0.28	-
Acarbose (Standard)	61.62 ± 0.26	95.45 ± 0.26

Molecular docking analysis

Molecular docking simulations were conducted to investigate the binding interactions of 44 kratom-derived compounds (**Table S(1)**) with α-glucosidase enzymes. The redocking of miglitol (PDB ID: 3L4W) and acarbose (PDB ID: 7DCH) was performed to

validate the docking protocol (**Figure 4**). The RMSD (root-mean-square deviation) values between the redocked and crystallographic poses were calculated using AutoDockTools. The RMSD values between the docked and crystallographic conformations were found to be 1.24 and 1.58 Å, respectively, supporting the reliability of the docking procedure (RMSD < 2.0 Å is considered acceptable). The binding energy (BE, kcal/mol) and the percentage of possible conformation or dock score (% DS) of all bioactive compounds were varying from –7.35 to –11.77 kcal/mol and 21% to 100%, respectively. The BE and %DS of selected bioactive compounds from *M. speciosa* are summarized in **Table 4**. The binding energies (BE) and cluster populations indicate the binding affinity and stability of the ligand-enzyme complexes. Miglitol and acarbose, known α- glucosidase inhibitors, were used as reference compounds. Acarbose exhibited stronger binding energies (−8.64 and −8.79 kcal/mol) than miglitol (−7.72 and −7.99 kcal/mol) against both enzymes, supporting its selection as the positive control in earlier *in vitro* α-glucosidase inhibition assays. Its robust docking score corresponds with its well-established mechanism as a competitive inhibitor at the active site.Several kratom-derived alkaloids and flavonoids exhibited stronger binding affinities than acarbose, suggesting potential inhibitory activity. Among the indole alkaloids, Mitrajavine (−10.89 and −11.77 kcal/mol) and Speciociliatine (−10.11 and −11.73 kcal/mol) showed the strongest binding to both enzyme isoforms. These compounds formed stable complexes with high cluster populations, indicating consistent docking poses. Oxindole alkaloids, particularly Stipulatine (−11.87 and −10.79 kcal/mol), Isorhynchophylline (−11.33 and −11.12 kcal/mol), and Speciofoline (−11.69 and −10.14 kcal/mol), demonstrated superior binding energies compared to both reference inhibitors. These compounds may contribute significantly to the enzyme inhibition activity of kratom extracts, especially given their high cluster stability (often >90%). The flavonols astragalin, hyperoside, and isoquercitrin showed moderate binding energies (−8.13 to −10.77 kcal/mol), with lower cluster populations. While their binding affinities are not as strong as alkaloids, they may provide synergistic antioxidant effects in kratom preparations [33]. The hydrogen bond interactions between the docked ligands and key catalytic residues of α-glucosidase, particularly Asp327 and Arg526. In the case of miglitol, hydrogen bonding and electrostatic interactions were identified with Asp327, Arg526, Asp542, and His600. For acarbose, similar interactions were observed with Asp327, Arg526, and His600, supporting its known role as a competitive inhibitor that mimics the substrate's transition state. These interactions have been shown to stabilize acarbose within the catalytic pocket, in agreement with previous crystallographic evidence. Although mitragynine exhibited a lower binding affinity, interactions with Arg526 and Asp542 through hydrogen bonding were detected. These findings suggest that partial occupation of the active site by mitragynine may occur though slightly less effectively than acarbose.

Although mitragynine did not exhibit the lowest binding energy among the tested compounds (–9.84 kcal/mol with 3L4W and –10.05 kcal/mol with 7DCH), it remains of particular pharmacological interest due to its high natural abundance in *M. speciosa* leaves and its well-established bioactivity profile. As the principal indole alkaloid, mitragynine often serves as a chemical marker and primary contributor to the biological effects of kratom extracts. Importantly, its experimental IC_{50} value of 48.09 µg/mL (120.70 µM) against α-glucosidase confirmed notable enzyme inhibition, exceeding the activity of the standard drug acarbose when measured in µg/mL. This suggests that mitragynine, despite having slightly weaker binding energy compared to other alkaloids, may possess favorable pharmacokinetic or structural characteristics that enhance its biological efficacy in a cellular context. Moreover, the presence of mitragynine in both the alkaloid extract and crude methanol extract, which also exhibited strong inhibitory activity, highlights its central role in the antidiabetic potential of kratom. Therefore, mitragynine may serve as both an active agent and a phytochemical scaffold for α-glucosidase inhibitors derived from natural products.

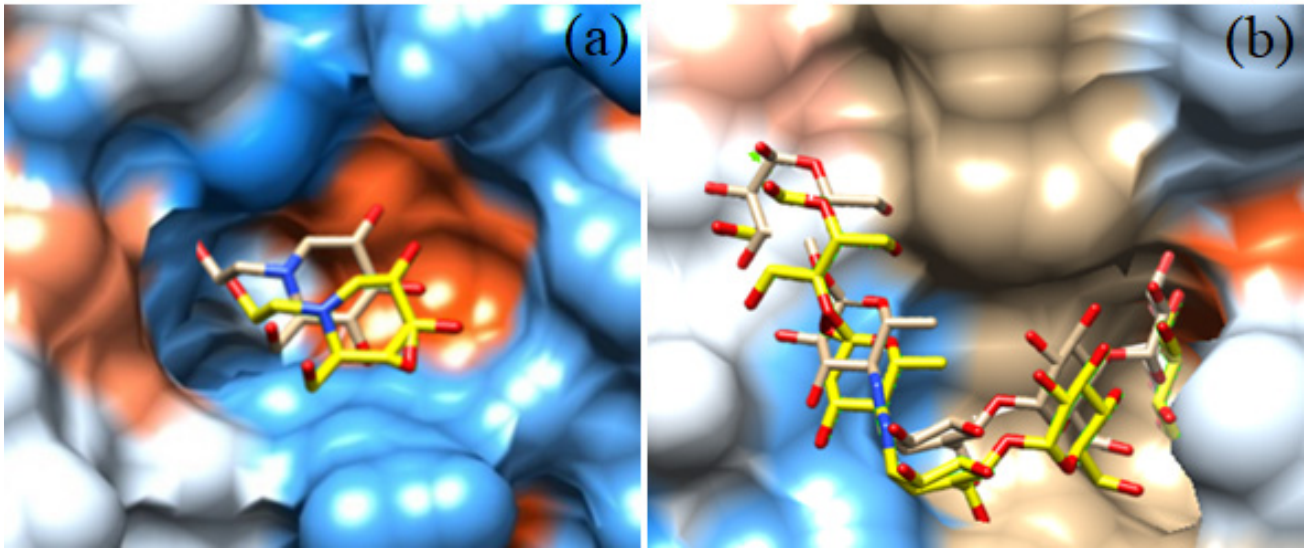

Figure 4 Superimposed binding poses of (a) miglitol with α-glucosidase (PDB 3L4W) and (b) acarbose with α-glucosidase (PDB 7DCH): X-ray structure (grey) and redocking pose (yellow).

Table 4 The BE and %DS of commercial drugs and selected most favorable *M. speciosa* compounds in the binding pocket of α-Glucosidase.

Structures from *M. speciosa* leaves	**Code**	**α-Glucosidase (3L4W)**		**α- Glucosidase (7DCH)**	
		BE (Kcal/mol)	***%DS***	**BE (Kcal/mol)**	***%DS***
miglitol		–7.72	99	–7.99	98
acarbose		–8.64	96	–8.79	98
Indole alkaloid					
Angustine	1	–7.9	100	–10.22	100
Ajmalicine	2	–9.12	63	–10.49	99
Akuammigine	3	8.33	99	–10.26	82
Mitrajavine	4	–10.89	59	–11.77	60
Corynantheidine	5	–10.52	88	–10.86	58
Hirsuteine	8	–7.35	56	–11.28	77
Mitraciliatine	9	–10.25	37	–11.31	69
Mitragynine	11	–9.84	53	–10.05	60
Paynantheine	12	–10.1	41	–11.14	81
Speciociliatine	13	–10.11	70	–11.73	86
7α-Hydroxy-7H-mitragynine	15	–9.4	33	–11.45	30
Mitragynaline	16	–8.83	69	–10.74	45
Oxindole alkaloid					
Isorhynchophylline	21	–11.33	100	–11.12	56
Isomitraphylline	23	–10.67	100	–10.08	100

Structures from *M. speciosa* leaves	Code	α-Glucosidase (3L4W)		α- Glucosidase (7DCH)	
		BE (Kcal/mol)	*%DS*	BE (Kcal/mol)	*%DS*
Mitrafoline	26	–10.27	59	–10.64	70
Isomitrafoline	27	–11.13	91	–10.87	55
Speciofoline	28	–11.69	68	–10.14	92
Stipulatine	30	–11.87	100	–10.79	46
Mitragynine oxidole A	31	–10.43	89	–10.13	37
Mitragynine oxidole B	32	-11.01	58	–10.71	64
Ciliaphylline	36	-10.43	37	–11.32	73
Flavonol					
Astragalin	62	–8.13	38	–10.38	18
Hyperoside	63	–8.33	21	–10.49	22
Isoquercitrin	65	–8.89	54	–10.77	23

Conclusions

This study presents a comprehensive comparative analysis of alkaloid and mitragynine content in *Mitragyna speciosa* leaves across different varieties, propagation methods, and leaf maturity stages. Among the 3 varieties examined - green vein, red vein, and "Hang Kang" - the Hang Kang variety propagated by seed and harvested at the semi-mature stage (4th leaf pair) exhibited the highest total alkaloid content (1.59 %w/w) and mitragynine concentration (10.37%, or 103.70 mg/g alkaloid extract). Taken together, these results underscore the dual importance of optimized cultivation parameters and phytochemical profiling in maximizing the industrial relevance of *M. speciosa*. The Hang Kang variety, particularly seed-propagated semi-mature leaves, offers a promising source of mitragynine for use in the development of bio-based functional compounds.

In vitro α-glucosidase inhibitory assays revealed that mitragynine exerted the strongest inhibitory activity (IC_{50} = 48.09 µg/mL), surpassing both the crude extracts and the reference drug acarbose on a weight basis. Molecular docking studies supported these results, showing favorable binding affinities of mitragynine and other kratom alkaloids with the α-glucosidase active site.

From an agricultural perspective, these findings suggest that selective cultivation of the Hang Kang variety using seed propagation may enhance mitragynine yields for commercial purposes. In terms of pharmacological development, the promising inhibitory activity of mitragynine supports its potential as a lead compound in antidiabetic drug research. Future studies should explore scaling up the optimized extraction protocol, structural modification of mitragynine analogs, and comprehensive *in vivo* evaluation of efficacy and safety.

Acknowledgements

This work was supported by National Higher Education, Science, Research and Innovation Policy Council, Thaksin University, Thailand (Fundamental Fund; FF-2567A105112017) Fiscal Year 2024 and Graduate Scholarship from Thaksin University, Thailand Research Fund. The authors would like to thank the Computational Chemistry Unit Cell, Faculty of Science, Chulalongkorn University, Thailand for providing research facilities, software packages, and computing times.

Declaration of Generative AI in Scientific Writing

During the preparation of this work the author(s) used ChatGPT in order to improve the readability and

language of the manuscript. After using this tool, the author(s) reviewed and edited the content as needed and take(s) full responsibility for the content of the publication.

CRediT Author Statement

Netnapa Chana: Conceptualization, Methodology, Supervision, Validation, and Writing –original draft.

Jamjan Pechsiri: Data curation, Formal analysis, Resources, and Visualization.

Parichat Thepthong: Data curation, Formal analysis, Resources, Validation, and Visualization.

Ratanaporn Pakee: Data curation, Validation, and Visualization.

Witsuta Decha: Data curation, Validation, and Visualization.

Panita Kongsune: Conceptualization, Methodology, Supervision, Validation, Software, Funding acquisition, and Writing –review & editing.

References

[1] T Begum, MH Arzmi, A Khatib, ABMH Uddin, MA Abdullah, K Rullah, SZ Mat So'ad, NFZ Haspi, MN Sarian, H Parveen, S Mukhtar and QU Ahmed. A review on *Mitragyna speciosa* (Rubiaceae) as a prominent medicinal plant based on ethnobotany, phytochemistry and pharmacological activities. *Natural Product Research* 2025; **39(6)**, 1636-1652.

[2] T Begum, MH Arzmi, MN Sarian, SAA Shah, SNH Azmi, ABMH Uddin, A Khatib and QU Ahmed. A review on multi-therapeutic potential of the *Mitragyna speciosa* (kratom) alkaloids mitragynine and 7-hydroxymitragynine: Experimental evidence and future perspectives. *Kuwait Journal of Science* 2025; **52(2)**, 100381.

[3] SC Eastlack, EM Cornett and AD Kaye. Kratom - pharmacology, clinical implications, and outlook: A comprehensive review. *Pain and Therapy* 2020; **9(1)**, 55-69.

[4] T Petcharat, T Sae-leaw, S Benjakul, TH Quan, S Indriani, Y Phimolsiripol and S Karnjanapratum. Extraction of kratom (*Mitragyna speciosa*) leaf compounds by enzymatic hydrolysis-assisted process: Yield, characteristics and its *in vitro* cytotoxicity in cell lines. *Process Biochemistry* 2024; **142**, 212-222.

[5] YS Goh, T Karunakaran, V Murugaiyah, R Santhanam, MHA Bakar and S Ramanathan. Accelerated solvent extractions (ASE) of *Mitragyna speciosa* Korth. (kratom) leaves: Evaluation of its cytotoxicity and antinociceptive activity. *Molecules* 2021; **26(3)**, 3704.

[6] W Innok, A Hiranrat, N Chana, T Rungrotmongkol and P Kongsune. *In silico* and *in vitro* anti-AChE activity investigations of constituents from *Mitragyna speciosa* for Alzheimer's disease treatment. *Journal of Computer-Aided Molecular Design* 2021; **35(3)**, 325-336.

[7] P Thepthong, S Srirat, W Hiranrat, P Kongsune and N Chana. Development of chitosan-based microencapsulation system for *Mitragyna speciosa* alkaloids: A novel approach for Alzheimer's disease treatment. *Journal of Pharmaceutical Innovation* 2025; **20(2)**, 58.

[8] S Suwanlert. A study of kratom eaters in Thailand. *Bulletin on Narcotics* 1975; **27(3)**, 21-27.

[9] LC Laforest, MA Kuntz, SRR Kanumuri, S Mukhopadhyay, A Sharma, SE O'Connor, CR McCurdy and SS Nadakuduti. Metabolite and molecular characterization of *Mitragyna speciosa* identifies developmental and genotypic effects on monoterpene indole and oxindole alkaloid composition. *Journal of Natural Products* 2023; **86(4)**, 1042-1052.

[10] P Tabboon, E Limpongsa, S Tuntiyasawasdikul, R Jarungsirawat, T Pongjanyakul and N Jaipakdee. Screening the potential of pharmaceutical liquids on enhancing dissolution, intestinal permeation, and stability of *Mitragyna speciosa* bioactive for peroral delivery systems. *Industrial Crops and Products* 2025; **225**, 120525.

[11] S Tuntiyasawasdikul, J Junlatat, P Tabboon, E Limpongsa and N Jaipakdee. *Mitragyna speciosa* ethanolic extract: Extraction, anti-inflammatory, cytotoxicity, and transdermal delivery assessments. *Industrial Crops and Products* 2024; **208**, 117909.

[12] M Jeddi, NE Hachlafi, ME Fadili, N Benkhaira, SH Al-Mijalli, F Kandsi, EM Abdallah, ZB Ouaritini, A Bouyahya, LH Lee, G Zengin, HN

Mrabti and KF Benbrahim. Antimicrobial, antioxidant, α-amylase and α-glucosidase inhibitory activities of a chemically characterized essential oil from *Lavandula angustifolia* mill.: *In vitro* and *in silico* investigations. *Biochemical Systematics and Ecology* 2023; **111**, 104731.

[13] P Zhang, W Wei, X Zhang, C Wen, C Ovatlarnporn and OJ Olatunji. Antidiabetic and antioxidant activities of *Mitragyna speciosa* (kratom) leaf extract in type 2 diabetic rats. *Biomedicine & Pharmacotherapy* 2023; **162**, 114689.

[14] NFZ Zailan, SNE Sarchio and M Hassan. Evaluation of phytochemical composition, antioxidant and anti-diabetic activities of *Mitragyna speciosa* methanolic extract (MSME). *Malaysian Journal of Medicine and Health Sciences* 2022; **18**, 93-100.

[15] T Limcharoen, P Pouyfung, N Ngamdokmai, A Prasopthum, AR Ahmad, W Wisdawati, W Prugsakij and S Warinhomhoun. Inhibition of α-glucosidase and pancreatic lipase properties of *Mitragyna speciosa* (Korth.) Havil. (kratom) leaves. *Nutrients* 2022; **14(19)**, 4094.

[16] FA Saddique, M Ahmad, UA Ashfaq, A Mansha, SG Khan. Alpha-glucosidase inhibition and molecular docking studies of 4-hydroxy-n'-[benzylidene/1-phenylethylidene]-2h-1,2-benzothiazine-3-carbohydrazide 1,1-dioxides. *Chiang Mai Journal of Science* 2021; **48(2)**, 460-469.

[17] F Hermawan, T Ernawati and S Kusumaningrum. A review on isolation, characterization, biosynthesis, synthesis, modification, pharmacological activities and toxicology of mitragynine. *Gazi University Journal of Science* 2024; **37(4)**, 1654-1672.

[18] N Leksungnoen, T Andriyas, Y Ku-Or, S Chongdi, R Tansawat, A Aramrak, C Ngernsaengsaruay, S Uthairatsamee, W Sonjaroon, P Thongchot, S Ardsiri and P Pongchaidacha. The effect of light intensity and polyethylene-glycol-induced water stress on the growth, mitragynine accumulation, and total alkaloid content of kratom (*Mitragyna speciosa*). *Horticulturae* 2025; **11(5)**, 573.

[19] S Chongdi, S Uthairatsamee, C Ngernsaengsaruay, T Andriyas and N Leksungnoen. Regional variability in growth and leaf functional traits of *Mitragyna speciosa* in Thailand. *International Journal of Plant Biology* 2025; **16(1)**, 52-60.

[20] N Leksungnoen, T Andriyas, C Ngernsaengsaruay, S Uthairatsamee, P Racharak, W Sonjaroon, R Kjelgren, BJ Pearson, CR McCurdy and A Sharma. Variations in mitragynine content in the naturally growing kratom (*Mitragyna speciosa*) population of Thailand. *Frontiers in Plant Science* 2022; **13**, 1028547.

[21] EM Mudge and PN Brown. Determination of mitragynine in *Mitragyna speciosa* raw materials and finished products by liquid chromatography with UV detection: Single-laboratory validation. *Journal of AOAC International* 2017; **100(4)**, 18-24.

[22] AB Jaykumar MHS Shihabudeen and K Thirumurugan. Screening of fifteen Indian Ayurvedic plants for alpha-glucosidase inhibitory activity and enzyme kinetics. *International Journal of Pharmacy and Pharmaceutical Sciences* 2011; **3(4)**, 267-274.

[23] L Sim, K Jayakanthan, S Mohan, R Nasi, BD Johnston, BM Pinto and DR Rose. New glucosidase inhibitors from an Ayurvedic herbal treatment for type 2 diabetes: Structures and inhibition of human intestinal maltase-glucoamylase with compounds from Salacia reticulata. *Biochemistry* 2010; **49(3)**, 443-451.

[24] K Wangpaiboon, P Laohawuttichai, SY Kim, T Mori, S Nakapong, R Pichyangkura, P Pongsawasdi, T Hakoshima and K Krusong. A GH13 α-glucosidase from Weissella cibaria uncommonly acts on short-chain maltooligosaccharides. *Acta Crystallographica Section D: Structural Biology* 2021; **77**, 1064-1076.

[25] FC Bernstein, TF Koetzle, GJ Williams, EFJ Meyer, MD Brice, JR Rodgers, O Kennard, T Shimanouchi and M Tasumi. The protein data bank: A computer-based archival file for macromolecular structures. *Journal of Molecular Biology* 1977; **112(3)**, 535-542.

[26] R Dennington, T Keith and J Millam. *GaussView, version 5*. Semichem Inc., Shawnee Mission, Kansas, 2009.

[27] MJ Frisch, M Frisch, G Trucks, K Schlegel, G Scuseria, M Robb, J Cheeseman, J Montgomery, T Vreven, KN Kudin, J Burant, J Millam, S Iyengar, J Tomasi, V Barone, B Mennucci, M Cossi, G Scalmani, N Rega, A Petersson, …, BA Johnson. *Gaussian 03, revision C02*. Gaussian, Inc., Wallingford, Connecticut, 2004.

[28] GM Morris, DS Goodsell, RS Halliday, R Huey, WE Hart, RK Belew and AJ Olson. Automated docking using a Lamarckian genetic algorithm and empirical binding free energy function. *Journal of Computational Chemistry* 1998; **19(14)**, 1639-1662.

[29] J Gasteiger and M Marsili. Iterative partial equalization of orbital electronegativity - a rapid access to atomic charges. *Tetrahedron* 1980; **36(22)**, 3219-3228.

[30] GM Morris, R Huey, W Lindstrom, MF Sanner, RK Belew, DS Goodsell and AJ Olson. AutoDock4 and AutoDockTools4: Automated docking with selective receptor flexibility. *Journal of Computational Chemistry* 2009; **30(16)**, 2785-2791.

[31] E Ermakova. Structural insight into the glucokinase-ligands interactions: Molecular docking study. *Computational Biology and Chemistry* 2016; **64**, 281-296.

[32] L Flores-Bocanegra, HA Raja, TN Graf, M Augustinović, ED Wallace, S Hematian, JJ Kellogg, DA Todd, NB Cech and NH Oberlies. The chemistry of kratom (*Mitragyna speciosa*): Updated characterization data and methods to elucidate indole and oxindole alkaloids. *Journal of Natural Products* 2020; **83(7)**, 2165-2177.

[33] W Innok, T Rungrotmongkol and P Kongsune. Insights into binding affinity of flavonoid compounds from Thai herbs against 2009 H1N1 hemagglutinin. *Trends in Sciences* 2022; **19(5)**, 2689.

Supplementary Material

Table S(1) List of bioactive compounds identified in mitragyna speciosa leaves and their functional groups.

Codes	Substance	Functional group
1	Angustine	Indole alkaloid
2	Ajmalicine	Indole alkaloid
3	Akuammigine	Indole alkaloid
4	Mitrajavine	Indole alkaloid
5	Corynantheidine	Indole alkaloid
6	Isocorynantheidine	Indole alkaloid
7	Hirsutine	Indole alkaloid
8	Hirsuteine	Indole alkaloid
9	Mitraciliatine	Indole alkaloid
10	Mitragynalic acid	Indole alkaloid
11	Mitragynine	Indole alkaloid
12	Paynantheine	Indole alkaloid
13	Speciociliatine	Indole alkaloid
14	Speciogynine	Indole alkaloid
15	7alpha-Hydroxy-7H-mitragynine	Indole alkaloid
16	Mitragynaline	Indole alkaloid
17	Mitralactonal	Indole alkaloid
18	Corynoxeine	Oxindole alkaloid
19	Corynoxine B	Oxindole alkaloid
20	Rhynchophylline	Oxindole alkaloid
21	Isorhynchophylline	Oxindole alkaloid
22	Mitraphylline	Oxindole alkaloid
23	Isomitraphylline	Oxindole alkaloid
24	Corynoxine	Oxindole alkaloid
25	Speciophylline	Oxindole alkaloid
26	Mitrafoline	Oxindole alkaloid
27	Isomitrafoline	Oxindole alkaloid
28	Speciofoline	Oxindole alkaloid
29	Isospeciofoline	Oxindole alkaloid
30	Stipulatine	Oxindole alkaloid
31	Mitragynine oxidole A	Oxindole alkaloid
32	Mitragynine oxidole B	Oxindole alkaloid

Codes	Substance	Functional group
33	Javaphylline	Oxindole alkaloid
34	Rhynchociline	Oxindole alkaloid
35	Isospecionoxeine	Oxindole alkaloid
36	Ciliaphylline	Oxindole alkaloid
37	Apigenin-7-O-glucoside	Flavone
38	Astragalin	Flavonol
39	Hyperoside	Flavonol
40	Quercitrin	Flavonol
41	Isoquercitrin	Flavonol
42	Quercetin-3-rhamnoside	Flavonol
43	Quercetin-3-galactoside-7-rhamnoside	Flavonol
44	Quercetin	Flavonol

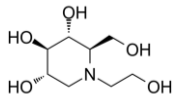
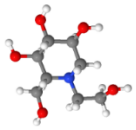

MOL : miglitol

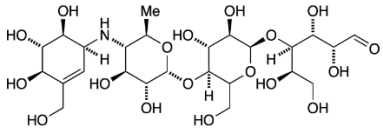
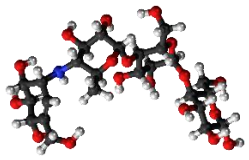

Acarbose

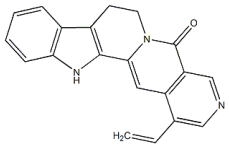
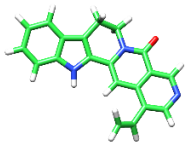
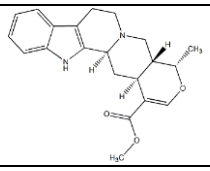
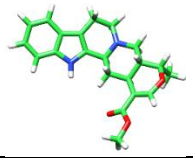

1 2

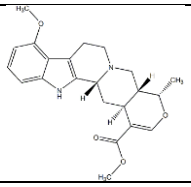
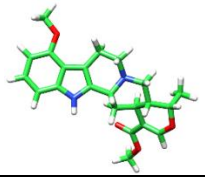
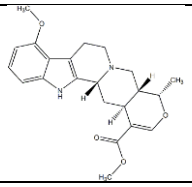
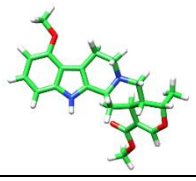

3 4

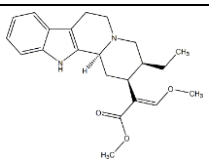
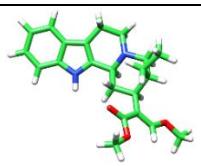
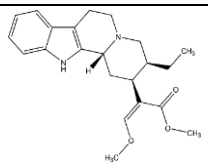
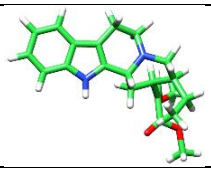

5 6

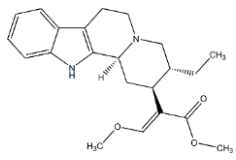

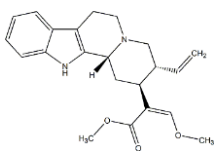
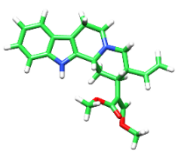

7 8

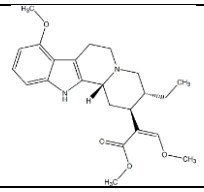
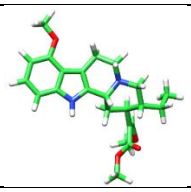
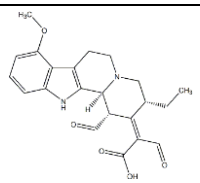
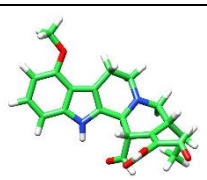

9 10

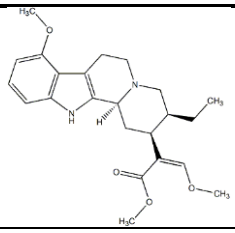
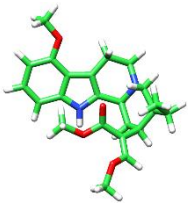
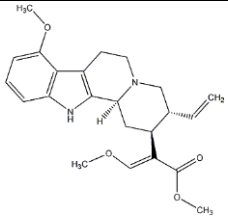


11 12

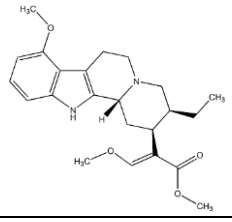

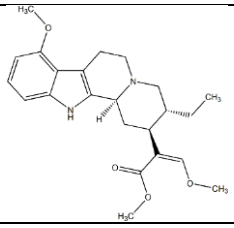


13 14

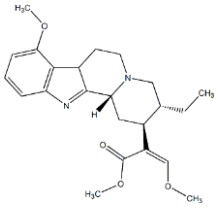
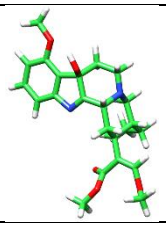
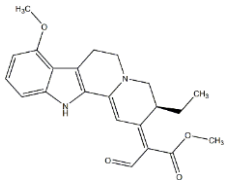
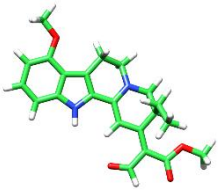

15 16

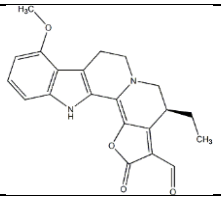
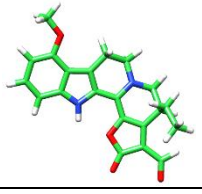
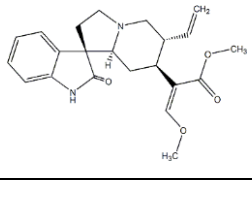
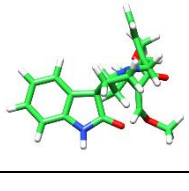

17 18

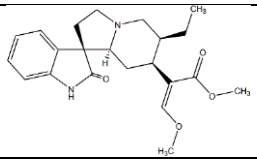
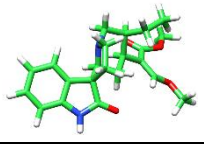
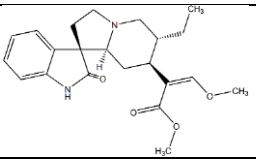
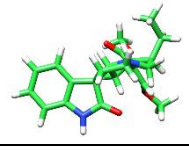

19 20

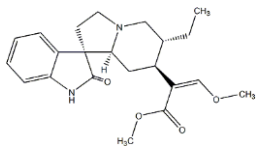
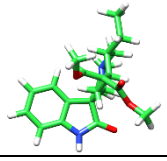

21

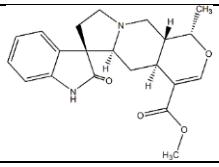
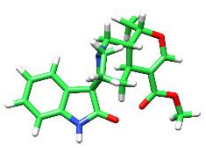

22

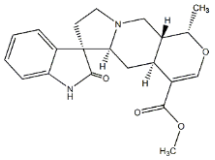
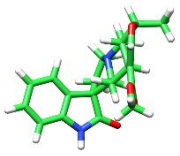

23

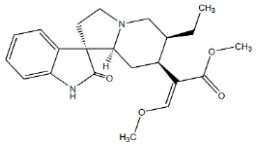


24

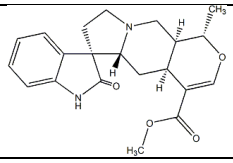
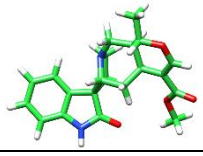

25

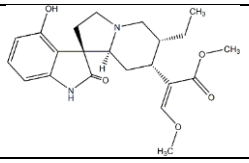


26

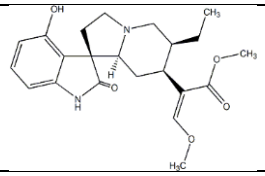
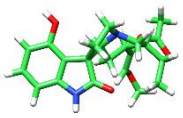

27

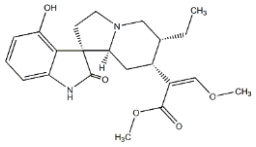


28

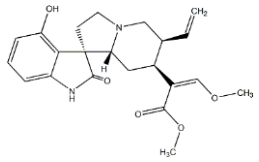
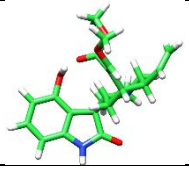

29

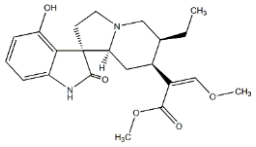


30

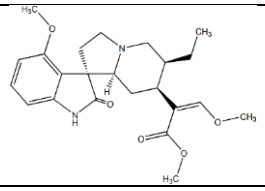
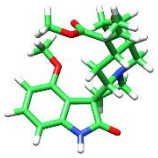

31

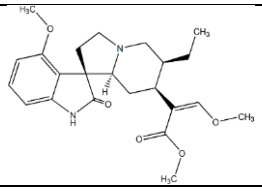
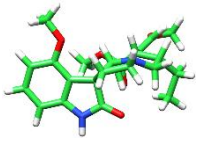

32

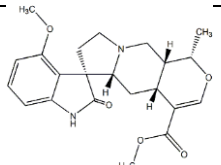


33

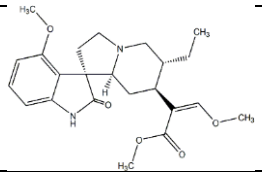
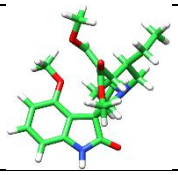

34

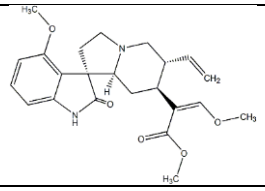
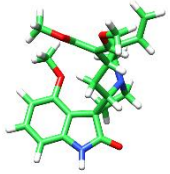

35

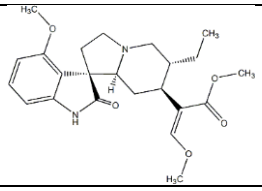
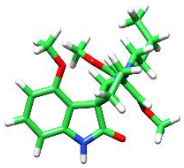

36

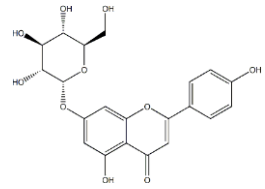		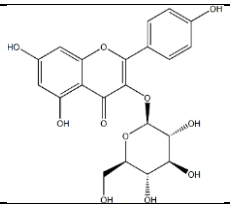	
37		38	
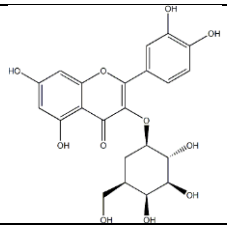	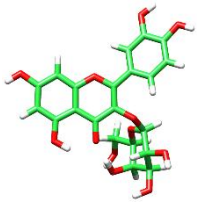	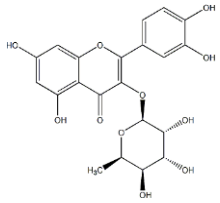	
39		40	
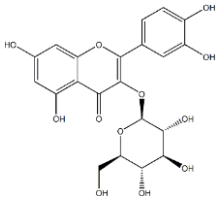	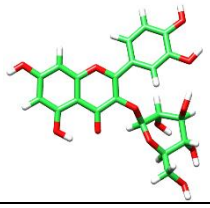	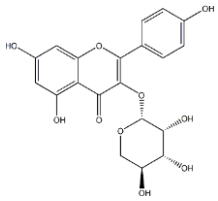	
41		42	
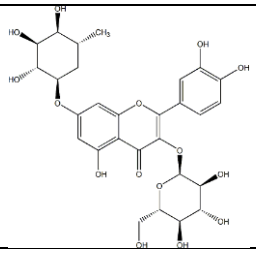	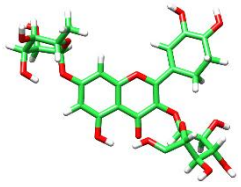	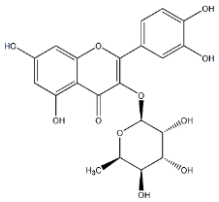	
43		44	